SEMARAK ILMU PUBLISHING

CFD Letters

Journal homepage:
https://semarakilmu.com.my/journals/index.php/CFD_Letters/index
ISSN: 2180-1363

3D Computational Fluid Dynamic Investigation on Wave Transmission behind Low-Crested Submerged Geo-Bag Breakwater

Ahmad Fitriadhy[1,*], Sheikh Fakruradzi[1], Alamsyah Kurniawan[2], Nita Yuanita[2], Anuar Abu Bakar[1]

[1] Faculty Ocean Engineering Technology and Informatics, Universiti Malaysia Terengganu, 21030, Kuala Terengganu, Terengganu, Malaysia
[2] Faculty of Civil and Environmental Engineering, Institut Teknologi Bandung, Indonesia

ARTICLE INFO

Article history:
Received 4 April 2023
Received in revised form 7 May 2023
Accepted 9 June 2023
Available online 1 October 2023

Keywords:
Submerged Breakwaters; Transmission Coefficients; Computational Fluid Dynamics; Experimental Tests; Wave Transformations

ABSTRACT

Wave transmission characteristics behind low-crested submerged breakwaters involve complex-hydrodynamic interaction of water waves on the structures. To properly comprehend the induced-nonlinear wave transformation, the problem necessitates a trustworthy prediction using a computational fluid dynamic (CFD) technique. The goal of this study is to develop a three-dimensional (3-D) computational model of the hydrodynamic performance of a narrow crest behind a submerged breakwater in order to gain a thorough understanding of the wave transmission coefficient, K_t. The simulation took into account a number of wave parameters such as wave steepness (H_i/L), relative submergence depth (H_i/h), and crest width (c_w/L) of the structure. A numerical wave flume model is included, which is based on the full Navier-Stokes solver and includes a shallow water model to account for nonlinearity in the incident wave field. In addition, laboratory measurements were also conducted using a geo-bag dike model as the main breakwater structure. The result shows that the reduction in transmission coefficient correlates highly with the wave steepness and the relative submergence and crest parameters. This can be attributed to most breaking waves over the submerged breakwater. The steeper the incident wave, the greater the reduction in the transmitted wave. And, the greater the principal dimensions of the breakwater, the greater the drop in transmission coefficient. For validation, the CFD results corroborate satisfactorily with measurements.

1. Introduction

Low-crested structures used to protect shorelines from severe erosion are known as submerged breakwaters. Due to demands for maintaining beach amenities and aesthetic values, submerged breakwaters have become an increasingly important use in recent years, particularly for recreational and residential coastal developments. The key fundamental knowledge behind the breakwater installation is that of capable dissipating a portion of incident wave energy as well induce insignificant environmental impacts on coastal seas, for example by allowing continuous refreshment of water flows across the structures. This inherent characteristic of submerged breakwaters may result in sufficient energy transformation and minimization of incident waves and thus wave transmission (K_t)

* *Corresponding author.*
E-mail address: naoe.afit@gmail.com (Ahmad Fitriadhy)

https://doi.org/10.37934/cfdl.15.10.1222

behind structures. Therefore, a complete investigation of the performance of a submerged breakwater under varied wave conditions to obtain a comprehensive insight into the characteristics of the wave transmission is necessarily required.

The wave breaking, overtopping, and associated turbulent effects over a low-crested submerged breakwater constitute a basic knowledge of the structural response and behaviour at diminishing wave transmission coefficient. In a physical model study, the transmitted wave was reduced by more than half of the incident wave predominantly because of boundary friction, breaking, and reflection (Hashim *et al.,* [1]). Chatchawin *et al.,* [2] discovered that the interaction of the sea dome with the generated incident wave reduces wave energy by approximately 50%. Similarly, the transmission coefficient, K_t minimizes to a range of values between 0.5 and 0.8 in an experimental test campaign on the rubble-mound detached breakwaters under typical real-life intense sea-storm conditions (Lorenzoni *et al.,* [3]). Despite several investigations, the wave attenuating effect of submerged breakwaters on reducing the attribute of K_t is still unknown, particularly beyond small waves, making it a fascinating research area.

Enormous literature in the field of submerged barriers had been mostly based on small-scale facilities (Dˊıaz-Carrasco *et al.,* [4]; Dieter and Peter, [5]; Niels *et al.,* [6]) and potential flow theory (Yong and Hua-Jun [7]; Mizutani *et al.,* [8]; Losada *et al.,* [9]), in which several hydrodynamic parameters were properly investigated. Experimental testing, on the other hand, is sometimes limited to a few aspects, making it difficult to measure some generated phenomena like turbulent dissipation and kinetic energy. Furthermore, the transmission coefficient, K_t, is affected by wave transformations caused by viscous and nonlinear processes such as vortices, turbulences, and boundary layer separation, which are not well explained by an ordinary mathematical model such as linear potential flow. Because the efficiency of a submerged breakwater is a result of complicated design parameters between waves and structural configuration, existing techniques are limited and may still fail to adequately characterize the nonlinear interaction effects between wave motion and submerged barriers.

Permeable breakwaters, such as rubble mounds and artificial reefs, are widely used in coastal engineering because they are mostly effective at reducing wave transmission and reflection (Huang *et al.,* [10]). According to a recent study, the nonlinear effects of porous medium induce a significant attenuation in the propagation of wave height and spatial velocities of approximately 30% and 50%, respectively, as quantified in an experimental investigation of oscillatory waves over porous bed (Corvaro *et al.,* [11]). A sufficient model, however, is needed for the breakwater's evaluation, where detailed information can be obtained from three-dimensional (3-D) analysis. Abdullah *et al.,* [12] studied 3-D wave transmission characteristics behind a Wave Breaker Coral Restorer (WABCORE) breakwater using computational fluid dynamic (CFD). They concluded that the model can reproduce satisfactorily the complex spatial distribution of induced turbulent energy resulting from wave breaking, overtopping, viscous friction, and drag across the breakwater boundary. Therefore, a complete flow field investigation in and around the permeable breakwater using reliable numerical methods cannot be omitted.

This paper presents an investigation of the hydrodynamic performance of wave transmission behind a submerged geo-bag breakwater numerically and experimentally. To achieve the objective, a computational fluid dynamic (CFD) approach has been conducted, which is then validated by laboratory measurement. Here, three-dimensional computational modelling is put forward to obtain a comprehensive insight into the characteristics of the transmission coefficient, K_t. The CFD model is employed using Reynolds Average Navier-Stokes (RANS) solver. For treating the highly nonlinear effect of wave interaction with this breakwater boundary, the shallow water model is introduced into the equations of fluid motion with the volume of fluid (VOF) method and turbulence model to capture

satisfactorily the generated wave transition in the neighbourhood of structure. Furthermore, a series of experimental studies for various wave conditions such as significant wave height, and peak period were carried out to produce significant results on the transmission coefficient, K_t. Several nonlinear effects of the wave field, such as wave profile characteristics, wave breaking and overtopping, and turbulent kinetic energy, are also reproduced. and explain elaborately with respect to the characteristics of K_t.

2. Computational Modelling Programme

2.1 Mathematical Model of Fluid Flow

The shallow water algorithm is used to simulate current fluid flow problems using the FLOW-3D application (Flow Science) [12], which is based on Reynolds Average Navier-Stokes (RANS) equations and turbulence closure model, as well as the volume of fluid approach. The reduced mass continuity equation for nonlinear, transient, and incompressible flow is rewritten as

$$(\nabla u A_x) + R(\nabla \mathfrak{w} A_z) + \xi \frac{(u A_x)}{x} = \frac{R_{SOR}}{\rho} \tag{1}$$

where u and $\mathfrak{w}$ are depth-averaged velocities referred to $x - z$ plane; V_f is the fractional volume open to flow; ρ is the fluid density; A is the fractional area of control volume open to flow; R_{SOR} is a mass source; R and ξ denotes the specified coefficients.

Then, the shallow water momentum equation in the horizontal plane is expressed as;

$$\frac{\partial U}{\partial_t} + \frac{1}{V_f}(UA\nabla U) = -\frac{1}{\rho}(\nabla p) + G + \frac{\tau_s + \tau_b}{\rho d} + 2\Omega U \tag{2}$$

where U is $(u, \mathfrak{w})$; ∇ is gradient operator; Ω is the vertical component of the earth's angular velocity; p is average fluid pressure; G is body acceleration; τ_s are the wind shear stress on a fluid surface, and τ_b are the bottom shear stresses, for x and z components. These shallow water equations form the basis of nonlinear fluid flow algorithms for simulating wave motion over a submerged barrier (see Figure 1). Referring to Fitriadhy *et al.,* [13] and Fitriadhy *et al.,* [14], the renormalized group (RNG) turbulence model was also applied in this study involving large eddies simulation (Reynolds number, Re > 10^3). This modified version of standard k_T-ε_T turbulence is considered as the most robust model in FLOW-3D that can produce fairly acceptable results for high Reynolds number (Jehad *et al.,* [15]). The two transport equations of the RNG turbulence model for the turbulent kinetic energy, and dissipation rate, ε_T are given as

$$\frac{\partial k_T}{\partial_t} + \frac{1}{V_f}\left\{u A_x \frac{\partial k_T}{\partial_x} + \upsilon A_y \frac{\partial k_T}{\partial_y} + \mathfrak{w} A_z \frac{\partial k_T}{\partial_z}\right\} = P_t + G_t + \mathrm{Diff}_{kt} - \varepsilon_T \tag{3}$$

$$\frac{\partial \varepsilon_T}{\partial_t} + \frac{1}{V_f}\left\{u A_x \frac{\partial \varepsilon_T}{\partial_x} + \upsilon A_y \frac{\partial \varepsilon_T}{\partial_y} + \mathfrak{w} A_z \frac{\partial \varepsilon_T}{\partial_z}\right\} = \frac{CDIS1 \cdot \varepsilon_T}{k_T}(P_t + \mathrm{CDIS3} \cdot G_t) + \mathrm{Diff}_{\varepsilon} - \mathrm{CDIS2}\frac{\varepsilon_T^2}{k_T} \tag{4}$$

where P_t is the turbulent kinetic energy production, G_t is the buoyancy production term whereas Diff_{kt} represents the diffusion term of kinetic energy. In Eq. (4), the $\mathrm{CDIS1}$, $\mathrm{CDIS2}$, and $\mathrm{CDIS3}$ denote the dimensionless parameters for the transport equation, and the $\mathrm{Diff}_{\varepsilon}$ is the diffusion of dissipation.

The transport equation of fluid fraction for tracking changes in the free surface of the water is expressed in Eq. (5),

$$\frac{\partial(F)}{\partial_t} + \overline{U}_m \cdot \nabla F = 0 \quad (5)$$

where $\overline{U}_m$ is the average velocity of the fluid, and F is the volume fraction of fluid.

2.2 Boundary Condition

Referring to Table 1, the wave boundary condition is assigned upstream on the left portion of the domain. In this boundary, the wavemaker generates regular waves into the computational domain according to specified wave theory. On the other end of the domain, the outflow boundary condition is applied downstream, in which a sponge layer is used to diminish the effects of wave reflection. On the lateral boundaries and other open boundaries, the symmetrical type boundary condition is used specifically to simulate nonlinearity in the shallow water waves passing over a submerged barrier.

Table 1
Boundary setting conditions

Description	Type	Condition
X_{min}	Wave	Far field
X_{max}	Outflow	Far field
Z_{min}	Symmetry	Far field
Z_{max}	Symmetry	Far field
Y_{min}	Symmetry	Far field
Y_{max}	Symmetry	Far field

Figure 1 shows the computational domain associated with shallow water boundary in the developed numerical wave tank.

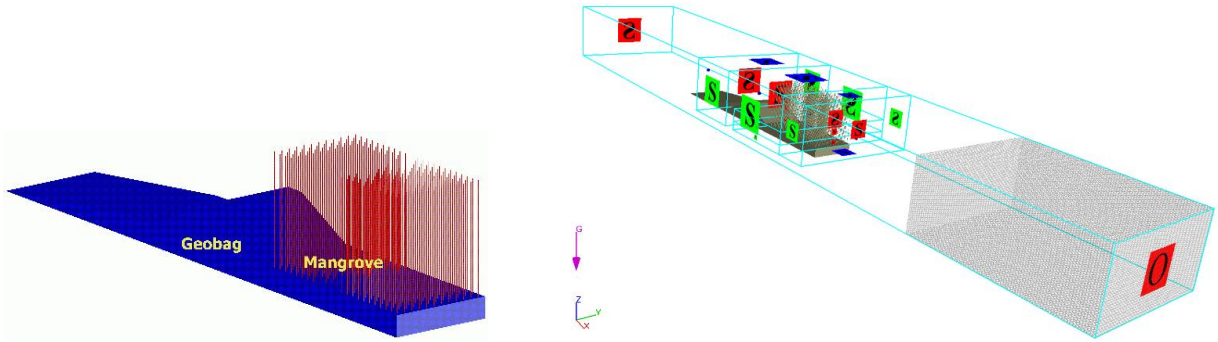

Fig. 1. Computational domain associated with shallow water boundary

2.3 Solution Schemes

The partial differential equations are solved using the finite difference method to derive the solutions of the unknown variables U, p, k_T, ε_T, and F from Eq. (1) to Eq. (5), where the time evolution of the unknown variables is advanced using the prescribed approach. The velocity components are initially approximated using Eq. (2) by ignoring the effects of pressure change for one computing cycle. This equation's advection terms are discretized using a second-order upwind method. The pressure field is then updated by modifying the approximated velocity components iteratively until it meets the continuity equation, Eq. (1). As a result, the predicted new velocity is revised to account for the effects of pressure changes. The turbulence field components k_T and ε_T are also computed from Eq. (3) and Eq. (4). Eq. (5) is used to update the new F-value for each cell on

the rectangular grid, and the new free surface configuration is reconstructed based on the F-value. Figure 2 shows this time evolution model of the forecasted surface elevation.

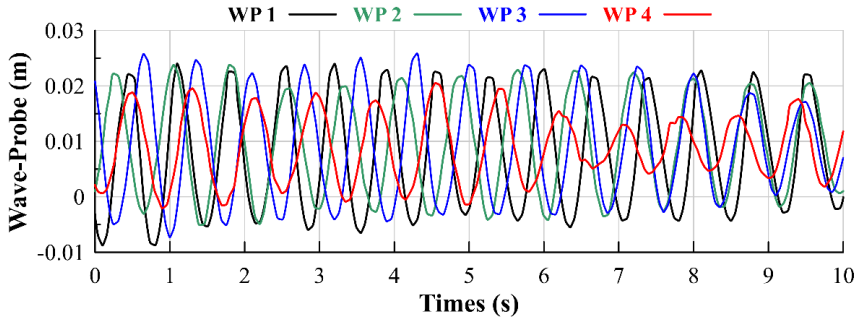

Fig. 2. Motion's Amplitude of Wave-Probe with Respect to Its locations

In addition, each step above applies the boundary conditions including rigid obstacle boundaries (for breakwater and mangroves) to modify the aforementioned fluid properties around the structures, as envisaged in Figure 3. The next cycles are then approximated by repeating all of these steps until the computational time is surpassed.

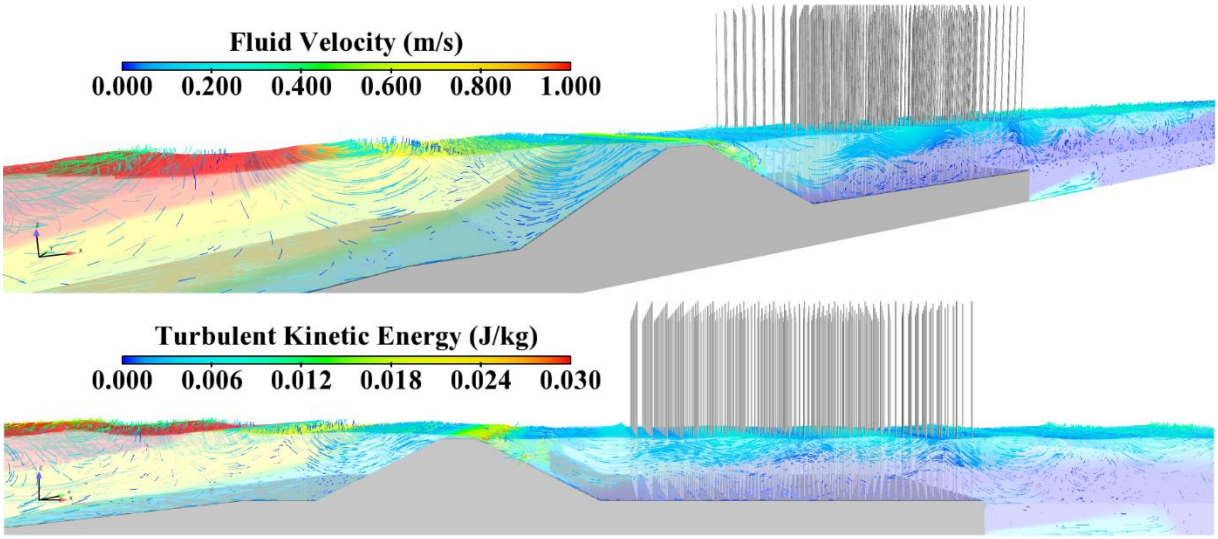

Fig. 3. CFD Visualisation of Hydrodynamic Characteristics Surrounding Geo-Bag and Mangrove Structures

3. Experimental Investigation

At the Ocean Engineering Laboratory of the Faculty of Civil and Environmental Engineering (FCEE), Institut Teknologi Bandung (ITB), a series of laboratory tests were conducted in a 2-D glass-walled flume. The main focus of this study is to assess the effectiveness of the geo-bag-dike in protecting juvenile mangroves. However, it is still necessary to incorporate the mangrove model to faithfully represent the real conditions of the natural coastal protection system. This inclusion is crucial because the study also aims to investigate the overall effectiveness of a coastal protection system. For this experiment, three different weight categories of geo-bag units were utilized: 0.5 kg, 1.0 kg, and 2.0 kg. These geo-bags were strategically positioned in the wave flume, creating a dike structure that adhered to a specific slope determined by the vertical to horizontal ratio. The geo-bags were arranged in the wave flume, forming a breakwater model switch with a front slope of 1:2. The

wave flume has a length of 40.0 m, a width of 1.2 m, and a height of 1.50 m, as illustrated in Figure 4.

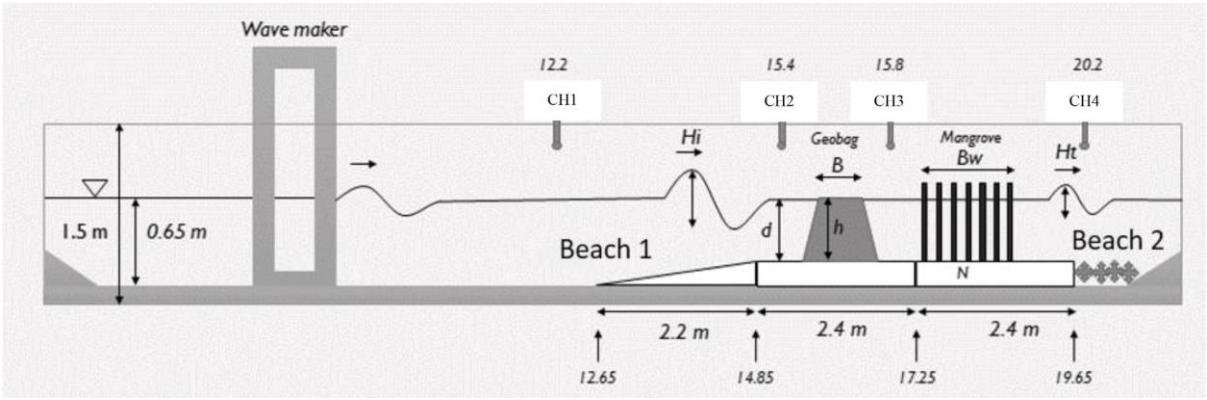

Fig. 4. Configuration of the physical model experiment on the wave flume

The wave flume's bottom is flat, and a wave paddle is mounted at the closed end to generate waves. Besides that, an absorbing beach model consisting of artificial mangroves made of iron bars and rubble mounds is utilized at the other end of the wave flume to lessen the effects of wave reflection. A submerged breakwater model is located approximately 16.05 m and 17.25 m respectively between the wave maker and the wave absorber. This submerged barrier was constructed from geo-bags which are made from canvas sacks filled with sand. Meanwhile, water depth (*d*) inside the flume was uniform with a depth of 0.65 m near the wave maker and 0.4 m in the beach area. The elevation of the breakwater crest was set to 0.0 cm MSL, that is, at the same level as the water surface.

In addition, CH1, CH2, CH3, and CH4 wave probes were installed at 12.2, 15.4, 15.8, and 20.2 meters down the flume from the wave paddle, respectively. The wave transmission coefficient is expressed as the ratio between transmitted wave height (H_t) and incident wave height (H_i).

$$K_t = H_t/H_i \tag{6}$$

The above equation holds an application for regular waves, however for irregular waves the transmitted wave energy can be used instead of the transmitted wave height (Goda and Suzuki [16]) as written in Eq. (7).

$$K_t = {H_t^2}\Big/{H_i^2} = {E_t}\Big/{E_i} \tag{7}$$

This equation is based on two presumptions. The first is that the energy of superposed waves (superposition of many linear component waves as discussed is actually the sum of the energies of individual wave trains. The second is that the representative wave heights being proportional to the square root of wave energy regardless of the directions of individual wave trains. Here, the transmitted wave height was obtained from the data of CH3. While the incident wave height was obtained from the CH2 wave probe. The effectiveness of the breakwater model was examined by varying the wave conditions and aforementioned geo-bag unit weights. Various wave conditions were generated against every scenario code, as indicated in Table 2. In this simulation, a series of individual random waves were generated by the wave maker, which was input based on the significant wave height and peak period using the JONSWAP distribution.

Table 2
Wave parameters for each wave condition

Code	**Significant wave height, H_s (m)**	**Peak period, T_p (s)**
W1	0.15	1.5964
W2	0.10	1.3034
W3	0.08	1.1658
W4	0.15	2.2576
W5	0.10	1.8433
W6	0.08	1.6487
W7	0.15	5.5300
W8	0.10	4.5152
W9	0.08	4.0386

4. Results and Discussion

The transmission coefficient results of computational fluid dynamics are presented in this section, as shown in Figures 5 to 8. The following subsections present the result discussions as well as appropriate CFD capture for the nonlinear-hydrodynamic phenomena such as wave breaking and overtopping over the breakwater model.

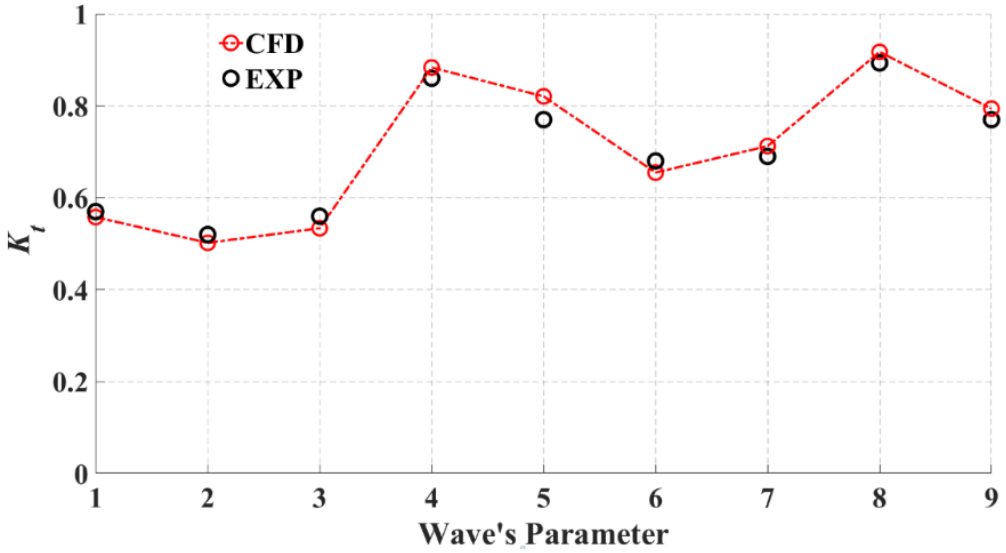

Fig. 5. Results comparisons between CFD and experimental measurements

4.1 CFD Verification

The change of transmission coefficient, K_t with various wave conditions is depicted in Figure 5. It is shown that K_t fluctuates over the entire range of the tested wave parameters, with minimum and maximum values of 0.502 and 0.917, respectively. The wave transmission coefficients increase (see W2 to W4 and W6 to W8) occurs due to decrease the effectiveness of the geo-bag (indicated by a higher transmission coefficient).

Nonetheless, the result shows that the CFD results agree qualitatively with the laboratory tests. Meanwhile, the discrepancies between CFD and the experimental data are approximately between 2.15% and 6.15% and do not basically deviate from the physical meaning of the hydrodynamic coefficient. A reason behind this favourable agreement can be attributed to the nonlinear-

hydrodynamic effects of wave interaction with the submerged breakwater using shallow-water modelling in large turbulent simulations.

4.2 Relative Wave Parameter

Figure 6 presents the relationship between transmission coefficient and designated wave properties such as wave steepness (H_i/L), relative submergence depth (H_i/h), and relative crest width (c_w/L) of the applied breakwater model. The results show that K_t tends to decrease rapidly with an increase in wave steepness and the relative structural width. In contrast, when the relative submergence depth increases, K_t tends to increase at a gradual rate. It is found in this study that the reduction in transmission coefficient correlates highly with the wave steepness and the relative structural parameters since most of the tested wave conditions lead to wave breaking over the submerged barrier.

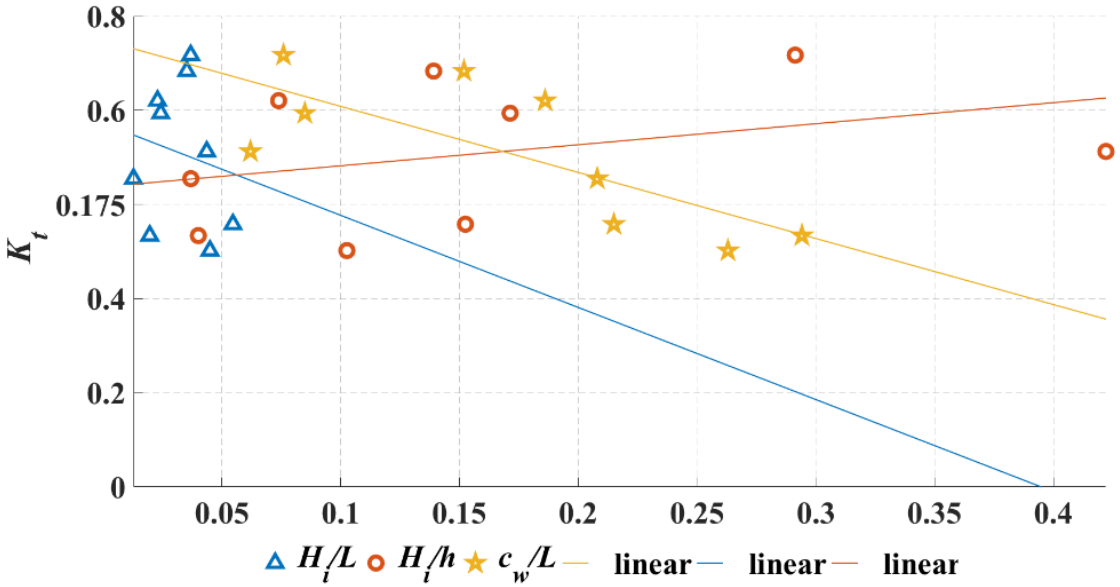

Fig. 6. Relationship between transmission coefficient and designated wave parameters

This is due to the fact that wave breaking and overtopping transform large portions of the mechanical energy of incident wave into turbulent kinetic energy, as indicated by the yellowish-red coloured pattern in Figure 7. Inherently, this magnifies the wave velocity at the lee-side of the geo-bag. In a series of numerical and experimental studies, Abdullah *et al.,* [12] discovered a significant wave transformation associated with wave breaking and overtopping in the vicinity of a submerged breakwater for increased relative wave parameters. In conclusion, the steeper the incident wave, the greater the reduction in transmitted wave height. And, the greater the principal dimensions of the breakwater, the greater the drop in transmission coefficient.

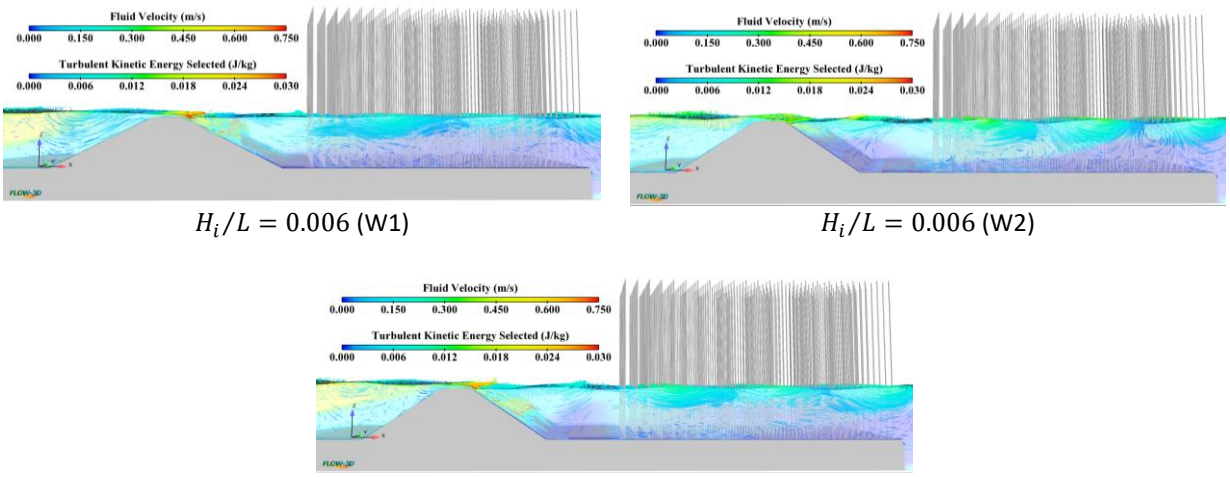

$H_i/L = 0.006$ (W1)

$H_i/L = 0.006$ (W2)

$H_i/L = 0.006$ (W3)

Fig. 7. CFD Visualisation of Hydrodynamic Characteristics Surrounding Geo-Bag and Mangrove Structures at Various Wave-Steepness

4.3 Relative Structural Parameter

The It is shown previously that the relative submergence depth (H_i/h), and relative crest width (c_w/L) of the submerged geo-bag breakwater have a significant correlation with the transmission coefficient because of most of the incident waves lead to wave breaking over a crown of the structure. Moreover, the construction cost of this submerged breakwater will increase exponentially with increased water depth. The above design problem, however, is not usually viewed as a complete design optimization problem where one optimum solution can be obtained that eventually improves the breakwater's performance and budgetary cost. On the other hand, in this subsection, the optimization curve of the structural systems is proposed.

Based on the numerical simulation, Figure 8 depicts the variations of transmission coefficient with the relative submergence depth and crest width parameters. The results have a high-degree nonlinear and continuous solution. Furthermore, the reproduced curves of H_i/h and c_w/L reveal that there is a near-optimal solution for the dimensional design of the relative submergence depth and the relative crest width of the breakwater structure. This design manipulation by taking an advantage of the optimization procedure can be very useful to control the transmission coefficient.

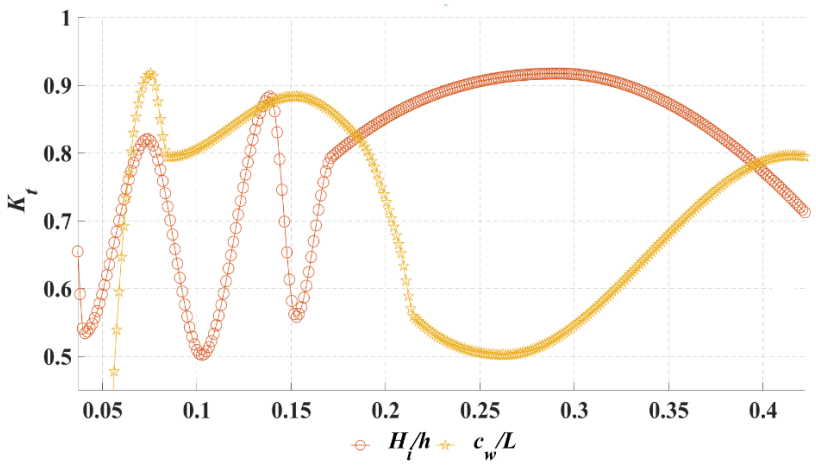

Fig. 8. Nonlinear results for transmission coefficient versus relative structural parameters

5. Conclusions

A 3D computational fluid dynamic investigation on the wave transmission coefficient, K_t behind a submerged geo-bag breakwater model was conducted in this study using Reynolds Average Navier-Stokes (RANS) solver. The numerical model includes modelling of the shallow water equations with the volume of fluid (VOF) method and turbulence model for treating the highly nonlinear effect of wave interaction with the breakwater boundary. In addition, a series of experimental studies for various wave conditions such as significant wave height, and peak period were carried out, in which the CFD results show a favourable agreement with the measurements.

The results reveal a significant correlation between the transmission coefficient, K_t, and the designated wave parameters such as wave steepness (H_i/L), relative submergence depth (H_i/h), and relative crest width (c_w/L) of the breakwater model. A reason is because of most waves break over a crown of the structure which eventually produces significant results of the transmitted wave. Future prospects of this innovative breakwater would be testing the model in the presence of forward and backward currents as well as evaluating the structure's effectiveness via an optimization procedure.

Acknowledgement
This research was funded by International Collaboration Research Grant between Institut Teknologi Bandung (ITB) and Universiti Malaysia Terengganu (UMT), VOT: 53507. The authors wish to greatly thank for Computer Simulation Laboratory, Faculty of Ocean Engineering Technology and Informatics, Universiti Malaysia Terengganu.

References

[1] Hashim, Ahmad Mustafa, Nur Diyana Md Noor, and Siti Nur Hanis Abdullah. "Wave Attenuation of Interlocking Concrete Unit-V (ICU-V)." *Applied Mechanics and Materials* 567 (2014): 313-318. https://doi.org/10.4028/www.scientific.net/AMM.567.313

[2] Srisuwan, Chatchawin, and Payom Rattanamanee. "Modeling of Seadome as artificial reefs for coastal wave attenuation." *Ocean Engineering* 103 (2015): 198-210. https://doi.org/10.1016/j.oceaneng.2015.04.069

[3] Lorenzoni, Carlo, Matteo Postacchini, Maurizio Brocchini, and Alessandro Mancinelli. "Experimental study of the short-term efficiency of different breakwater configurations on beach protection." *Journal of Ocean Engineering and Marine Energy* 2, no. 2 (2016): 195-210. https://doi.org/10.1007/s40722-016-0051-9

[4] Díaz-Carrasco, Pilar, Mª Victoria Moragues, María Clavero, and Miguel Á. Losada. "2D water-wave interaction with permeable and impermeable slopes: Dimensional analysis and experimental overview." *Coastal Engineering* 158 (2020): 103682. https://doi.org/10.1016/j.coastaleng.2020.103682

[5] Vanneste, Dieter, and Peter Troch. "2D numerical simulation of large-scale physical model tests of wave interaction with a rubble-mound breakwater." *Coastal Engineering* 103 (2015): 22-41. https://doi.org/10.1016/j.coastaleng.2015.05.008

[6] Jacobsen, Niels G., Marcel RA van Gent, and Guido Wolters. "Numerical analysis of the interaction of irregular waves with two dimensional permeable coastal structures." *Coastal Engineering* 102 (2015): 13-29. https://doi.org/10.1016/j.coastaleng.2015.05.004

[7] Liu, Yong, and Hua-Jun Li. "Analysis of wave interaction with submerged perforated semi-circular breakwaters through multipole method." *Applied Ocean Research* 34 (2012): 164-172. https://doi.org/10.1016/j.apor.2011.08.003

[8] Mizutani, Norimi, Ayman M. Mostafa, and Koichiro Iwata. "Nonlinear regular wave, submerged breakwater and seabed dynamic interaction." *Coastal Engineering* 33, no. 2-3 (1998): 177-202. https://doi.org/10.1016/S0378-3839(98)00008-8

[9] Losada, I. J., R. Silva, and M. A. Losada. "3-D non-breaking regular wave interaction with submerged breakwaters." *Coastal Engineering* 28, no. 1-4 (1996): 229-248. https://doi.org/10.1016/0378-3839(96)00019-1

[10] Huang, Ching-Jer, Hsing-Han Chang, and Hwung-Hweng Hwung. "Structural permeability effects on the interaction of a solitary wave and a submerged breakwater." *Coastal engineering* 49, no. 1-2 (2003): 1-24. https://doi.org/10.1016/S0378-3839(03)00034-6

[11] Corvaro, S., E. Seta, A. Mancinelli, and M. Brocchini. "Flow dynamics on a porous medium." *Coastal Engineering* 91 (2014): 280-298. https://doi.org/10.1016/j.coastaleng.2014.06.001

[12] Abdullah, Sheikh Fakhruradzi, Ahmad Fitriadhy, and Safari Mat Desa. "Numerical and experimental investigations of wave transmission behind a submerged WABCORE breakwater in low wave regime." *Journal of Ocean Engineering and Marine Energy* 7 (2021): 405-420. https://doi.org/10.1007/s40722-021-00209-8

[13] Fitriadhy, Ahmad, Nur Amira Adam, Nurul Aqilah Mansor, Mohammad Fadhli Ahmad, Ahmad Jusoh, Noraieni Hj Mokhtar, and Mohd Sofiyan Sulaiman. "CFD Investigation into The Effect of Heave Plate on Vertical Motion Responses of a Floating Jetty." *CFD Letters* 12, no. 5 (2020): 24-35. https://doi.org/10.37934/cfdl.12.5.2435

[14] Fitriadhy, Ahmad, Nurul Aqilah Mansor, Nur Adlina Aldin, and Adi Maimun. "CFD analysis on course stability of an asymmetrical bridle towline model of a towed ship." *CFD Letters* 11, no. 12 (2019): 43-52.

[15] Jehad, D. G., G. A. Hashim, A. Kadhim Zarzoor, and CS Nor Azwadi. "Numerical study of turbulent flow over backward-facing step with different turbulence models." *Journal of Advanced Research Design* 4, no. 1 (2015): 20-27.

[16] Goda, Yoshimi, and Yasumasa Suzuki. "Estimation of incident and reflected waves in random wave experiments." In *Coastal Engineering 1976*, pp. 828-845. 1976. https://doi.org/10.1061/9780872620834.048